Structural Development of TMMA and SSQXN-8 as Porous Chelating Resins

Gehan M. Ibrahim, Mohamed I. Ahmad, Belal El-Gammal

Atomic Energy Authority, Hot Laboratories Center, P.O. 13759, Cairo, Egypt

Received 28 July 2008; accepted 11 January 2009
DOI 10.1002/app.30042
Published online 4 May 2009 in Wiley InterScience (www.interscience.wiley.com).

ABSTRACT: Superfast kinetics of Nd^{+3}, Eu^{+3}, and Gd^{+3} ions were studied on the surfaces of *N, N, N`, N`*-tetramethylmalonamide (TMMA) and silsesquioxane (SSQXN-8) resins. TMMA and SSQXN-8 were prepared by suspension polymerization and sol–gel routes, respectively. They were identified using elemental analysis, FTIR, H-NMR, ^{13}C-NMR, MIP, and BET surface area. Kinetic investigations were performed in batch conditions and different models were used to fit the data; Boyd and Helfferich models were found the best. The diffusion of the ions through the resins were very fast and found to be in the order of 10^{-16} m^2/S. Effective diffusions of the studied ions were found to be 10^{-15} order of magnitude and directly proportional to the kinetic energy of the transition state. ΔS^* values from -166.044 to -179.297 J mol^{-1} K^{-1} were estimated as entropy stability factors of the system. © 2009 Wiley Periodicals, Inc. J Appl Polym Sci 113: 3038–3048, 2009

Key words: lanthanides; superfast kinetics; TMMA; SSQXN-8; spectroscopy and diffusion

INTRODUCTION

In recent years, there has been significant interest in the studies of both alkyl substituted amides[1] and oligomeric polyhedral silsesquioxanes[2–4] as alternatives to organophosphorus extractants and resins, respectively. They are less detrimentally degraded either radiolytically or hydrolytically than organophosphorus compounds.[1] In an advantage, they are completely incinerable, which implies that the amount of secondary wastes generated during waste treatment could be significantly reduced.[5]

Some organophosphorus compounds, namely, dihexyl-*N*,*N*-diethylcarbmoylmethyl-phosphonate and *n*-octyl(phenyl)-*N*,*N*-isobutylcarbamoylphosphine oxide have been used for the removal of some actinide and lanthanide species from acidic radioactive waste tanks.[6] Some chelating resins have been developed based on chemical bond formation between the phosphorus-containing compounds and the main chain of the base resin.[7,8] However, the bond formation of these products was not assessed. Moreover, the disadvantages of phosphorus-containing resins[9] led some researchers to synthesize alternative resins.[6,7] Their work was restricted to uranyl and cerium species and limited to their kinetic studies.[6,9]

In case of oligomeric polyhedral silsesquioxane compounds, styrene was connected to the silsesquioxane by substitution of only a single monostyryl group (St-Si$(Cl)_3$) to three hydroxyl groups in the silsesquioxane core (3Si-OH)[10]. Other researchers used glycol with organosilanes to synthesize inorganic–organic silsesquioxane and silica.[11] These materials, glycolate, and styryl-silsesquioxane offer limited functionality, which is not favored in radioactive waste treatment.[5]

This study introduces multidimensional structural investigations of TMMA and SSQXN-8 resins in the nanoscale level using different tools with multidimensional exchange kinetics of some lanthanides.

EXPERIMENTAL

Preparation of TMMA resin

Anhydrous dimethylformamide (DMF), 99.9%; 4-chloromethylstyrene (CMS) and sodium hydride (NaH) were purchased from Fluka Chemical Company, Germany, whereas 1, 4-divinyl benzene (DVB) was supplied by BDH, UK.

The following sketch by Nogami et al., 2003, represents the synthesis of TMMA resin (Fig. 1).[6,12] It was synthesized by the conventional suspension polymerization of 1, 4 divinyl benzene and 4-chloromethyl styrene. A surfactant (dodecane, Sigma-Aldrich grade solvent, USA) was used as a pore producing solvent at 70°C for 18 h. The obtained copolymer particles were washed with bidistilled water

Correspondence to: B. El-Gammal (belalelgammal@hotmail.com).

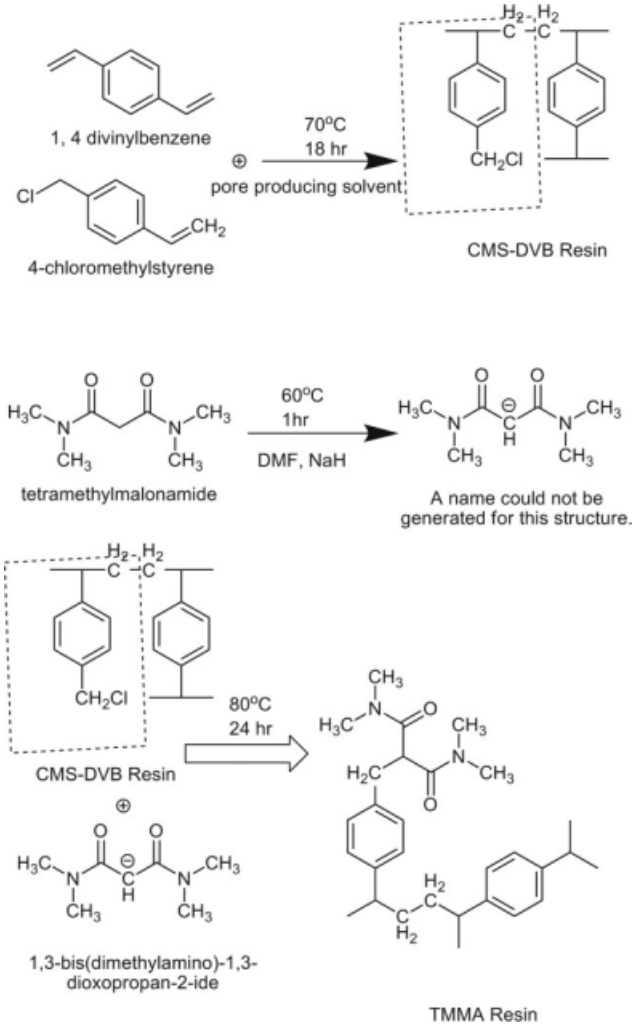

Figure 1 Preparation sketch of TMMA resin.[6,12]

and acetone, and then sieved to different mesh sizes. *N*`,*N* tetramethylmalonamide was treated with NaH in presence of DMF for partial dehydration of the central methylene group at 60°C for 1 h under N_2 atmosphere. The formed 1,3-bis(dimethylamino)-1,3-dioxopropan-2-ide was latter reacted with CMS-DVB copolymer to form TMMA resin end product. The reactants were heated at 80°C for 24 h with continuous stirring using magnetic stirrer. The final product was vacuum dried at room temperature then characterized using different techniques.

Preparation of SSQXN-8 resin

3-Chloropropyltriethoxysilane (CPTES), 97%; hydrochloric acid, 36.7%; ethanol, 99.9% were purchased from Fluka Chemical Company, Germany, whereas 3-amino-1, 2, 4-triazole (ATZ) was purchased from Sigma–Aldrich Chemical Company, USA, that were used with no extra purification.

According to the scheme described in Figure 2, ethanol was used as a solvent during the hydrolysis CPTES in presence of HCl as a catalyst, by stirring ethanol and CPTES (16 : 1) in 5 L volumetric flask and purging N_2 gas in the flask. The prepared 3-dichloropropylsilsesquioxane was then allowed to react with 0.3 moles of ATZ with refluxing the whole mixture for 15 h. A yellow precipitate of 3(3-amino-1, 2, 4-triazole)propylsilsesquioxane, ATZSSQXN-8 was obtained, which is filtered, washed with DMF and ethanol and vacuum dried for 24 h.

Characterization of the resins

Elemental analysis of TMMA &SSQXN-8 resins was achieved using CHNSO flash analyzer, Model EA

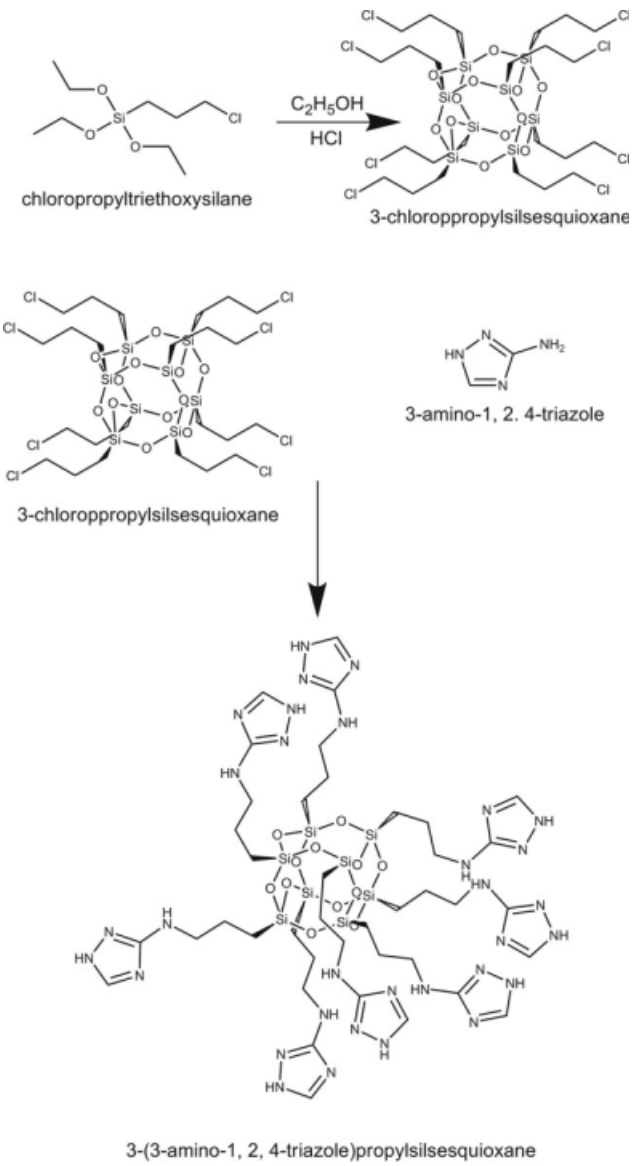

Figure 2 Preparation sketch of SSQXN-8 resin.

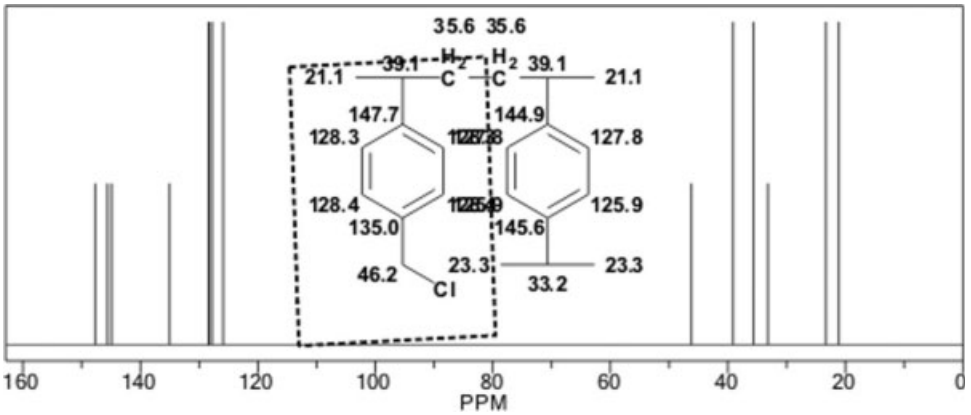

Figure 3 ^{13}C-NMR spectrum of DVB-CMS.

1100 Series, Finnigan Company, U.S.A. The silicon content of SSQXN-8 resin was assayed gravimetrically by calcination of the resin between 500°C–900°C.

The ^{1}H-NMR and ^{13}C-NMR spectra of the resins were collected using solid-state NMR spectroscopy technique, by means of Bruker DRX, 500 MHz Spectrometer, BRUKER BioSpin Group, USA.

The different porosities of the different TMMA and SSQXN-8 resins were measured by mercury intrusion porosimetery (MIP), using Micromeritics 9320 Pore Size Analyzer.

N_2 adsorption–desorption isotherms were constructed at 77 K after outgassing the resins for 3 h in a simultaneous heat-degassing unit, directly connected to a NOVA3000 Series Surface Analyzer, Quantachrom, USA. The BET surface area was experimentally evaluated from the adsorption branch of the isotherm in P/P_o range between 0.5 and 0.35. Post to adsorption, the pore types, and shapes were determined from the linear part of the t-plots, whereas their distribution was calculated using the BJH model.

The functionality on TMMA and SSQXN-8 resins were tested by measuring their FTIR Spectra using Perkin Elmer Spectrometer, BXII, Perkin Elmer Corporation, USA.

Adsorption properties

As reported, gadolinium, europium, and neodymium oxides, Fluka products, Germany, were used in the preparation of the corresponding nitrates.[13] Batch adsorption experiments were performed in HNO_3 medium for the obtained nitrates solutions containing 100 mg/L of the specified ion, loaded on 25 mg of the resin. At 25°C, batch adsorption time profiles were measured by the determination of the concentrations of Nd^{3+}, Eu^{3+}, and Gd^{3+} spectrophotometrically, in aqueous solutions using Arsenazo-III reagent.[14,15]

RESULTS AND DISCUSSION

The two resins were characterized using advanced techniques to evaluate them kinetically with different models.

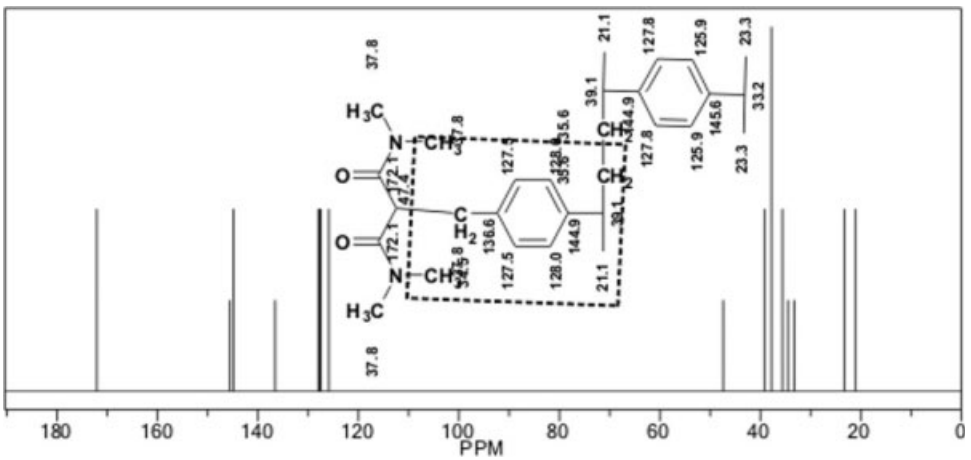

Figure 4 ^{13}C-NMR spectrum of TMMA resin.

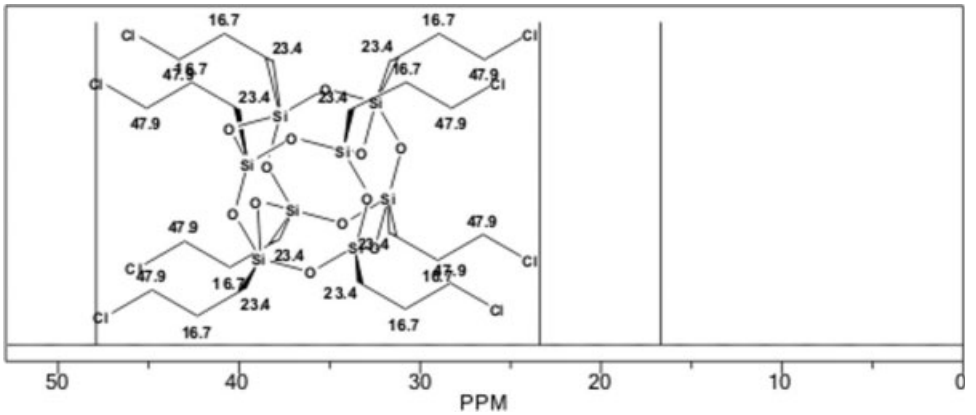

Figure 5 ^{13}C-NMR spectrum of CPSSQXN.

Characterization of the prepared TMMA and SSQXN-8 resins

Infra red transmission spectra

The FTIR spectrum of TMMA resin indicated that two distinct peaks at about 1580 and 1485 cm^{-1} were observed, which may be attributed to deformation modes of the double bond of the benzene ring. Other peaks were observed at about 3080 and 1690 cm^{-1}, which may be assigned to C—H stretching and carbonyl deformation modes, whereas broad band was observed at 3490 cm^{-1} because of free H_2O molecules. These results are in agreement with others in literature.[6,12]

The summarized FTIR spectrum of SSQXN-8 showed that two weak bands were observed at about 1310 and 1430 cm^{-1}, which may be attributed to single C—N bond deformation modes. On the other hand, the double C=N bond of the triazole ring is clearly watched after deformation at about 1700 cm^{-1}. Other single beaks were identified at about 1620 cm^{-1} (N—H), 2940 cm^{-1} (weak C—H) and 3430 cm^{-1} (broad deformation of OH group in water molecules). The more attractive feature of the FTIR spectrum is clearly observed due to symmetric stretching of Si—O—Si bond at about 780–1100 cm^{-1} and the absence of Si—H deformation peak at about 2250 cm^{-1}, which indicates that a complete substitution of the triazole group on the eight vertices of the SSQXN-8 core.[16]

Carbon-13 nuclear magnetic resonance spectroscopy

Beside elemental analysis, ^{13}C-NMR was used for elucidation of molecular structures of TMMA and SSQXN-8 resins. This task had been achieved by tracking the ^{13}C-NMR of the reacting components and the final end product resins.

Figure 3 shows the ^{13}C-NMR spectra of DVB-CMS and their predicted chemical shifts on vertices of the assigned structures. Thirteen peaks were observed, whereas 15 are predicted. For benzene rings, δ 135.1,

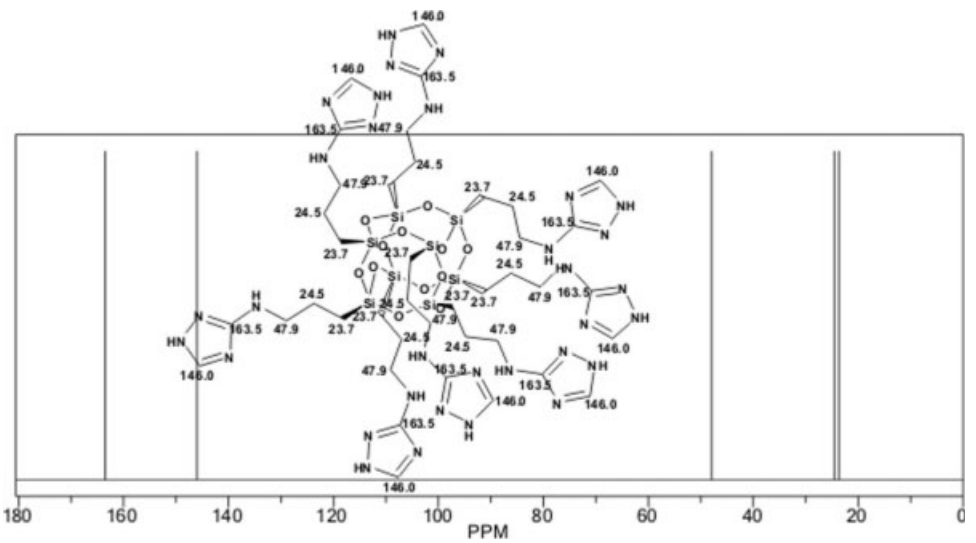

Figure 6 ^{13}C-NMR spectrum of SSQXN resin.

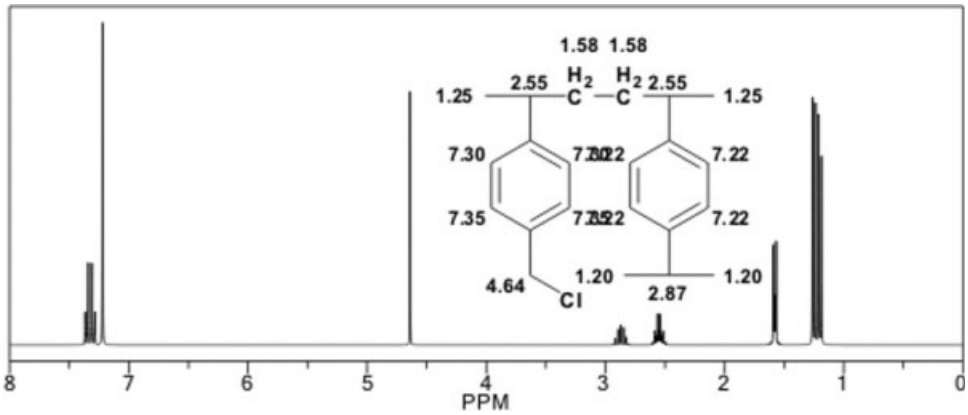

Figure 7 ^{1}H-NMR spectrum of DVB-CMS.

128.5, 145.7, 125.8, 144.1, and 127.2 ppm were assigned to the two benzene rings, whereas δ 39.2, 33.2, 35.4, and 46.4 ppm could be attributed to the aliphatic parts of DVB-CMS. The latter band at 46.4 ppm was shifted 37.9 ppm as a result of replacement of Cl atom by 1.3-bis (dimethylamino)-1,3-dioxopropan-2-iole group on preparation of the TMMA resin as shown in Figure 4. Also, two bands were detected at 172.2 and 37.8, which reveal the presence of carbonyl and methyl groups in the TMMA resin.

Figures 5 and 6 show the ^{13}C-NMR spectra of CPSSQXN and SSQXN-8, respectively. The aliphatic C atoms were assayed at low frequencies, namely, at δ 16.6 for the C—C—Cl group, which disappeared on replacement of the terminal Cl atom with the ATZ group with NMR shift to 24.4 ppm. Moreover, two distinct peaks at 146.2 and 164 ppm of the heterocyclic nucleus were observed.

Proton nuclear magnetic resonance spectroscopy

Figures 7 and 8 show that DVB-CMS gives three signals for the aliphatic H atoms, namely, m (1.23 ppm), d-1.56, p-2.54 ppm. The 4th signal at 4.65 may be attributed to the presence of lower shielding from the chlorine atom to the adjacent C—H atoms. For the 2-benzene rings, three doublets were observed at 7.21 ppm (1st ring) and 7.36 & 7.31 ppm (2nd ring). The latter values have been shifted to higher shielding at d-7.0 and d-7.25 ppm, respectively, as a result of formation of the TMMA resin. Also, the s-4.65 (4th aliphatic signal) have changed to d-3.47 ppm.

As seen in Figures 9 and 10, t-0.59, p-1.6, and t-3.69 ppm were detected by the spectrometer for CPSSQXN. On SSQXN-8 formation the t-3.69 was shifted to q-3.34 because of higher shielding also, weak s-7.62, s-13.5 signals of the ATZ were detected.

Kinetic testing

The adsorption of Nd^{+3}, Eu^{+3}, and Gd^{+3} ions from 100 ppm of the corresponding nitrate aqueous solutions were studied as a function of time using the batch technique. The obtained results are plotted as ion uptake by resin versus time. Figures 11–16 show that the mentioned three lanthanide ions experienced a superfast kinetics when compared with other organic and inorganic resins[17–19]; a fraction of an hour is sufficient to maintain equilibrium. Also, it can be observed from these figures that the rate of

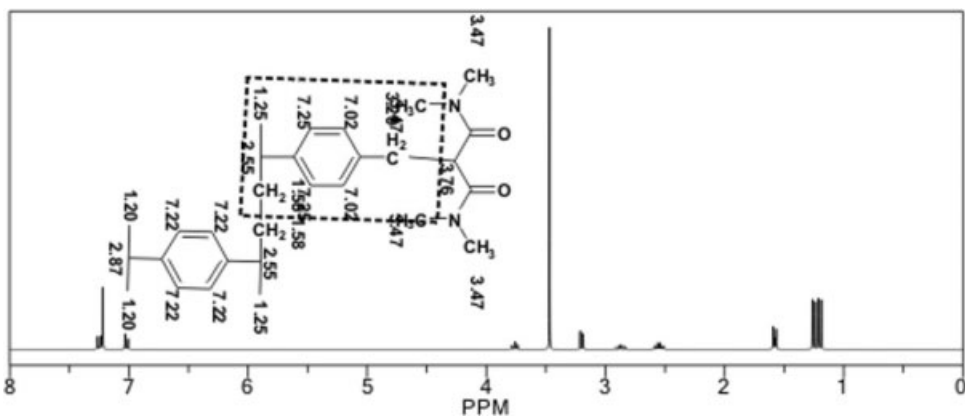

Figure 8 ^{1}H-NMR spectrum of TMMA resin.

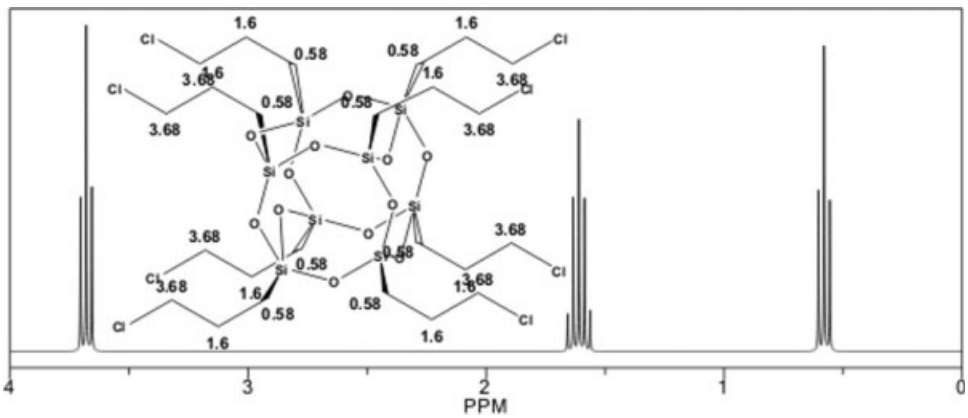

Figure 9 ^{1}H-NMR spectrum of CPSSQXN.

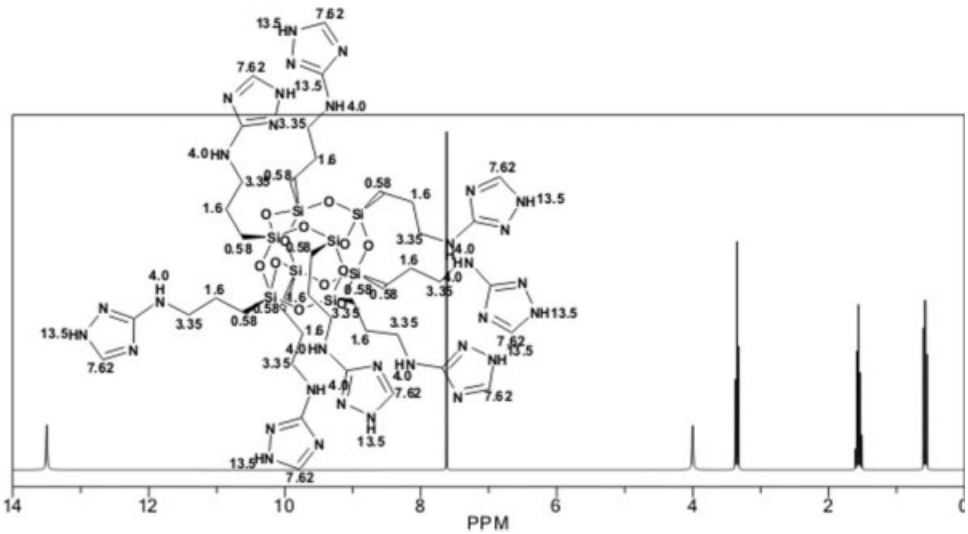

Figure 10 ^{1}H-NMR spectrum of SSQXN-8.

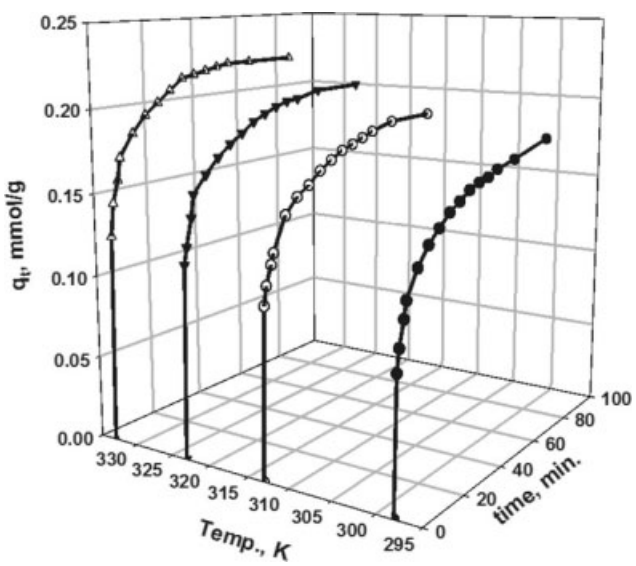

Figure 11 Adsorption time profile of Eu^{3+} on TMMA resin at different reaction temperatures.

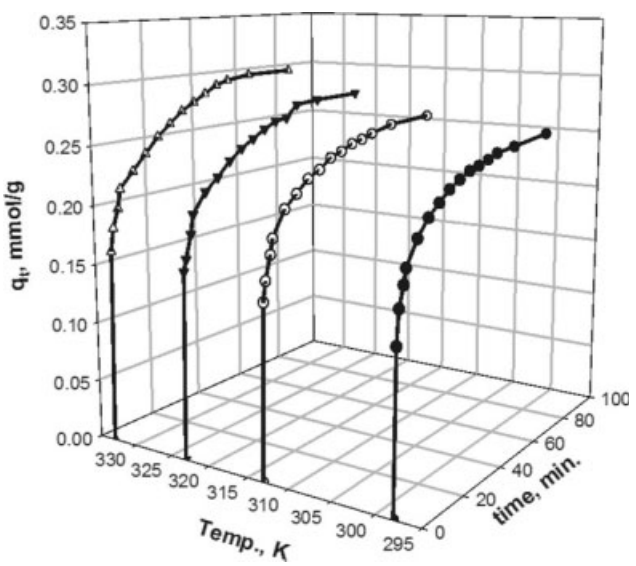

Figure 12 Adsorption time profile of Gd^{3+} on TMMA resin at different reaction temperatures.

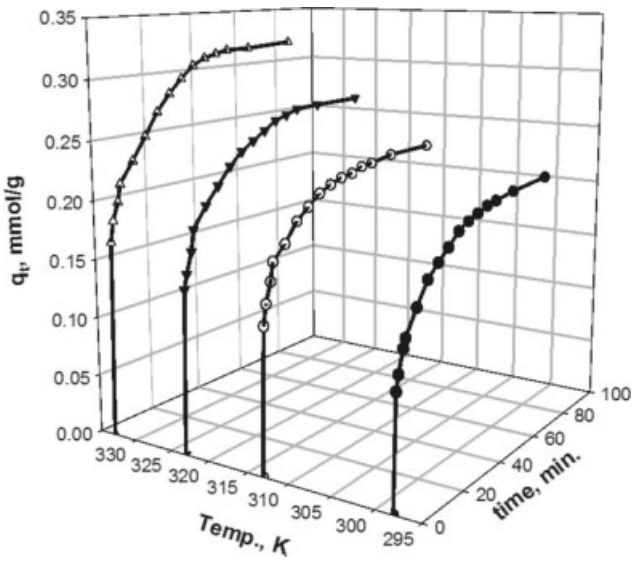

Figure 13 Adsorption time profile of Nd^{3+} on TMMA resin at different reaction temperatures.

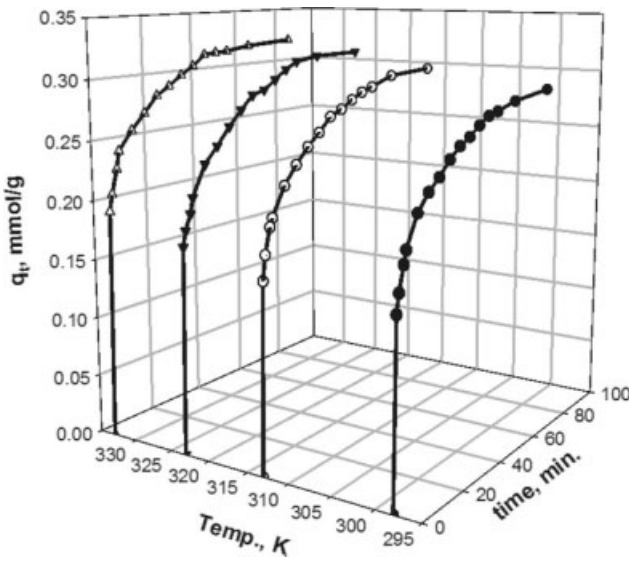

Figure 15 Adsorption time profile of Gd^{3+} on SSQXN-8 resin at different reaction temperatures.

uptake of any ion by the SSQXN-8 resin is faster than that the corresponding TMMA one; the order of the rates have increased with increasing the reaction temperature. This indicates the endothermic nature of the sorption process. The difference in ion removal between the two resins may be attributed to the difference in both the surface properties and surface nature of the solid. SSQXN-8 has a specific surface area as 862 m^2/g and 1.6 mL total pore volume, whereas TMMA possessed 328 m^2/g surface and 1.23 mL total pore volume. Moreover, the pore fractionation of the two solids showed that in SSQXN-8 micropore filling with Nd^{+3}, Eu^{+3}, and Gd^{+3} ions has been reached, while ink bottle-shaped mesopore filling was observed according to BJH models and IUPAC classifications.[20]

As reported earlier,[12] the adsorption of ions onto solid ion exchange resins or chelating resins must be considered as a liquid/solid phase reaction. Such type of reactions include the diffusion of reacting ions from solution to the resin surface, diffusion within the solid resin beads and possible chemical reactions between the ions and the functional groups of the resin. The sorption kinetics is governed by the slowest of these processes.

The kinetic models and the rate equations for the above cases have been established and are well presented by Helfferich.[12,21] If the diffusion of ions from

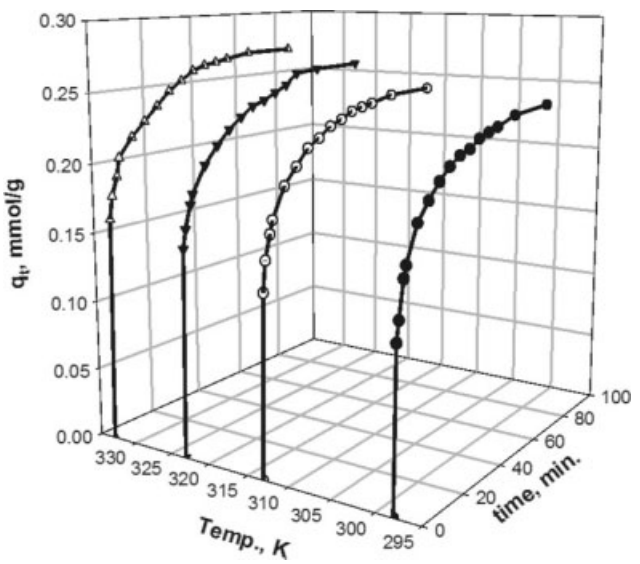

Figure 14 Adsorption time profile of Eu^{3+} on SSQXN-8 resin at different reaction temperatures.

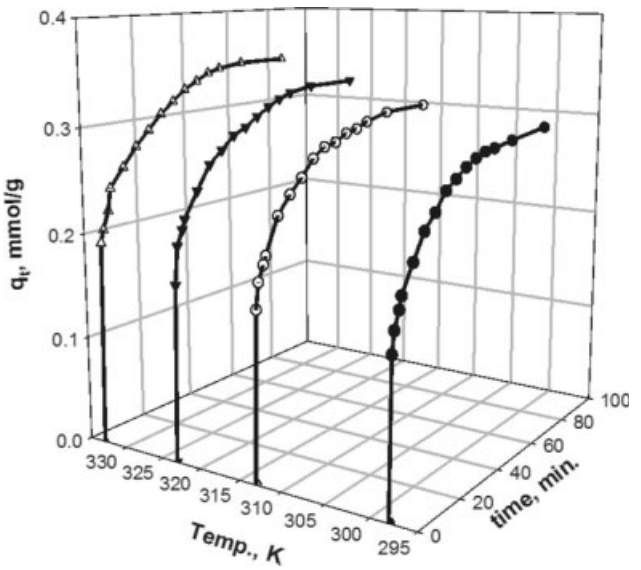

Figure 16 Adsorption time profile of Nd^{3+} on SSQXN-8 resin at different reaction temperatures.

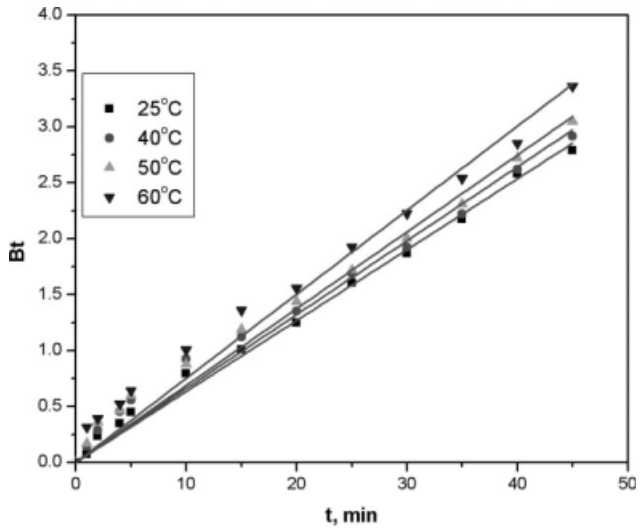

Figure 17 Helfferich plots of Nd^{3+} sorbed onto SSQXN-8 resin at different reaction temperatures.

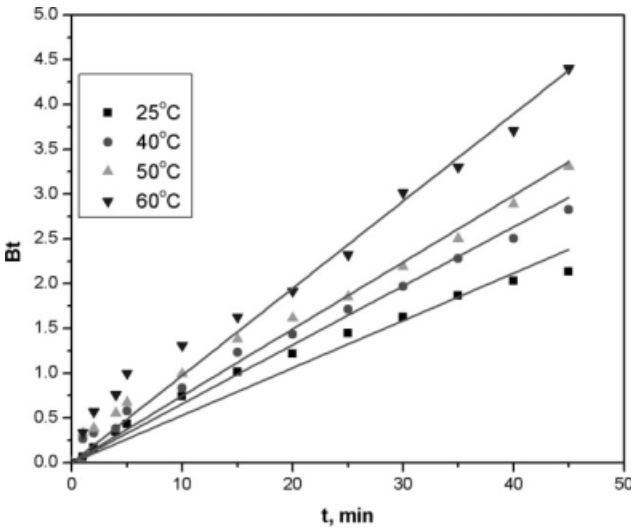

Figure 19 Helfferich plots of Eu^{3+} sorbed onto TMMA resin at different reaction temperatures.

the solution to the resin surface is the slowest step, the liquid film diffusion model controls the rate of adsorption. In such case, the following relation can be used to calculate the diffusion coefficient:

$$1 - F = \exp\left(\frac{-3D_i t}{rk\Delta r}\right) \tag{1}$$

where D_i is the diffusion coefficient, F is the uptake fraction, r is the radius of the solid particle, k is the equilibrium concentration of a certain ion or species in the resin divided by the concentration of the same species in solution, and Δr is the thickness of the liquid film. Therefore, D_i can be calculated from the slope of the plotting of *log(1−F)* versus time.

On the other hand, eq. (2) is hold when the diffusion of ions through the resin beads is the slowest step. In this case, the particle diffusion will be the rate-determining step and D_i could be calculated from the particle diffusion model expressed as

$$F = 1 - \left(\frac{6}{\pi}\right)\sum_{n=1}^{\infty}\frac{1}{n^2}\exp^{\left(-\frac{D_i\pi^2 n^2 t}{r^2}\right)} \tag{2}$$

where n is integers 1, 2, 3,.... If B is defined as

$$B = \frac{D_i\pi^2}{r^2}$$

It follows that

$$F = 1 - \left(\frac{6}{\pi}\right)\sum_{n=1}^{\infty}\frac{1}{n^2}\exp^{(-Btn^2)} \tag{3}$$

According to eqs. (1) and (3), the two models were tested; film diffusion models failed to interpret the results, clearly when low correlation coefficients were noticed.

Particle diffusion mathematical treatment [eq. (3)] was used to fit the experimental data as shown in Figures 17–22. In these Figures, the mathematical function, B could be fairly obtained. Arrhenius plots (Fig. 23) are then used to estimate activation energy, E_a, and the effective diffusion coefficient, D_o, for forward calculation of the change in entropy of activation, ΔS^*, as reported in eq. (4) by Barrer et al.[22] as

$$D_o = 2.72\frac{\kappa T d^2}{h}e^{\Delta S^*/R} \tag{4}$$

where k, h, and T refer, respectively, to Boltzman constant, Planck's constant, absolute temperature and the average distance between two successive

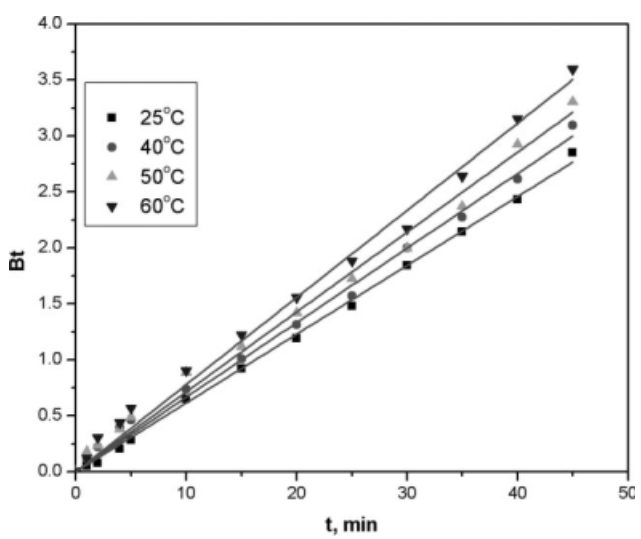

Figure 18 Helfferich plots of Nd^{3+} sorbed onto TMMA resin at different reaction temperatures.

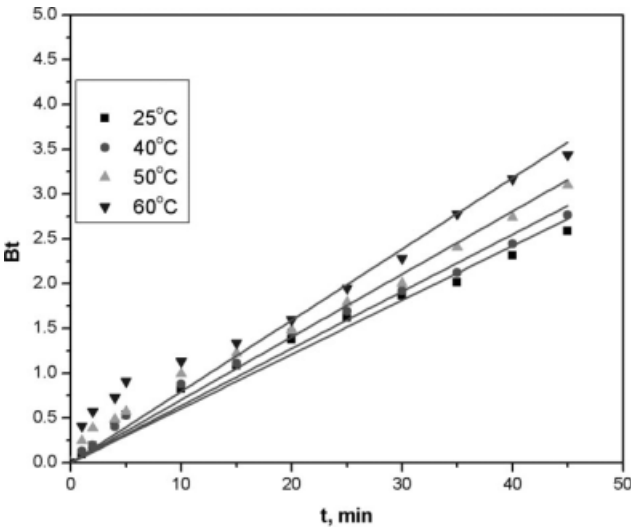

Figure 20 Helfferich plots of Eu^{3+} sorbed onto SSQXN-8 resin at different reaction temperatures.

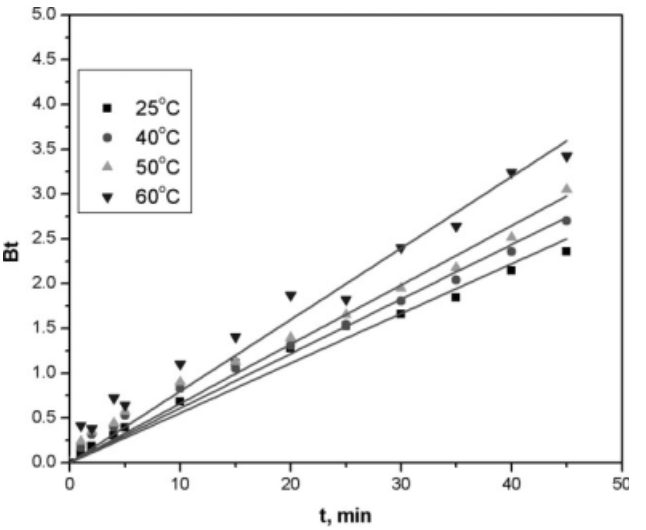

Figure 22 Helfferich plots of Gd^{3+} sorbed onto SSQXN-8 resin at different reaction temperatures.

positions in the process of diffusion, which was taken as 0.5 mm. The calculated D_i, D_o, E_a, and ΔS^* values are given in Table I.

The rate of exchange of different ions on either TMMA or SXQXN-8 resin is independent of their solution concentrations to certain extent and the rate of exchange was found to increase with decrease in particle size. In other aspect, linear relationship between the mathematical function, B and the inverse square of the particle radius is hold for the metal ions under study; 0.5×10^{-6} m average particle size was used in the remaining work. These observations support the particle diffusion control under the set conditions and are in agreement with some reports found in ion exchange systems.[23–27]

The diffusion coefficients for all ions sorbed on the two resins lies in the 10^{-16} orders of magnitude. On the other hand, 10^{-15} orders of magnitude are characteristic for self-effective diffusion coefficients of the ions in the system. This assures the predominance of particle diffusion mechanism in the two different functional resins; one may act as a cation exchanger (SSQXN-8), while coordination is expected to participate for TMMA.[6]

It can be also noted that the diffusion coefficient of $Eu^{3+}/H^+ > Gd^{3+}/H^+ > Nd^{3+}/H^+$. This can be attributed to the difference in mobility of the ion in solution; smaller ions tend to travel faster through the bulk of the particle by increasing the reaction temperatures.[12,28,29] A similar observation was found in preconcentration of some lanthanides in some chelating resins.[12]

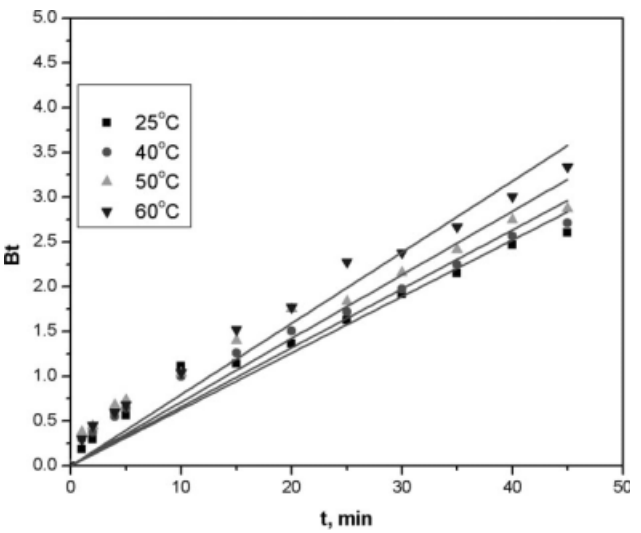

Figure 21 Helfferich plots of Gd^{3+} sorbed onto TMMA resin at different reaction temperatures.

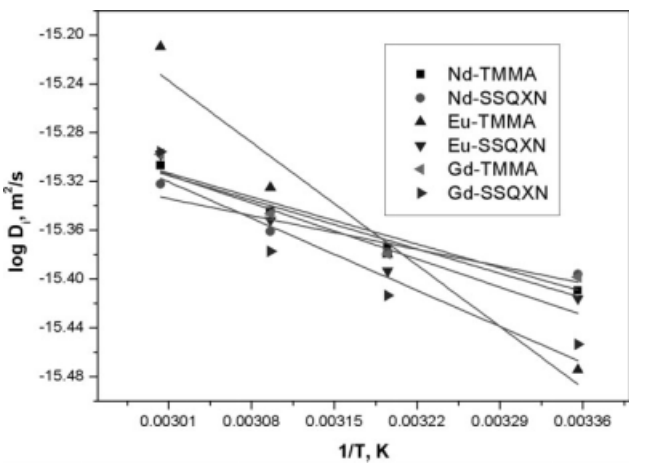

Figure 23 Variation of diffusion coefficients of Nd^{3+}, $Eu3^+$, and Gd^{3+}on TMMA and SSQXN-8.

TABLE I
Diffusion and Thermodynamic Parameters of Activation of Some Lanthanides at Different Reaction temperatures

	$D_i \times 10^{16}$ (m^2/s)					
	Nd^{3+}		Eu^{3+}		Gd^{3+}	
Diffusion coefficient	TMMA	SSQXN-8	TMMA	SSQXN-8	TMMA	SSQXN-8
Temperature (°C)						
25	3.89579	4.01876	3.35383	3.83747	3.99594	3.52054
40	4.22160	4.18674	4.17153	4.04158	4.17470	3.86029
50	4.52396	4.35408	4.73060	4.44980	4.50558	4.19371
60	4.93471	4.7642	6.1733	5.04057	5.03867	5.06275
Self diffusion coefficient	$D_o \times 10^{15}$ (m^2/s)					
	3.50127	1.81645	8.40861	4.69417	3.29284	8.94436
Activation energy	E_a (kJ/mol)					
	2.380886	1.646215	5.979078	2.730988	2.30198	3.520322
Entropy of activation	ΔS^* (J $mole^{-1}$ K^{-1})					
	−173.841	−179.297	−147.413	−171.404	−174.352	−166.044

The E_a values of transition state trivalent lanthanide ions reflect their superfast kinetics; a maximum kinetic energy of 5.9 kJ/mol is observed in case coordination of Eu^{3+} with TMMA resin, whereas only 1.64 kJ/mol was obtained of Nd^{3+} ion sorption on SSQXN-8. This phenomenon explains the faster diffusion of the remaining ions on the SSQXN-8 resin rather than TMMA one; less E_a values and more negative entropy changes were calculated for SSQXN-8 resin. This may assigned to the difference in their specific surface area and porosities. The ΔS^* values mainly varies with the extent of hydration of the exchangeable ion, i. e., any change in water structure around ions that may occur when they pass through the channels of exchanger particles. The negative values obtained for the entropy of activation suggest that no significant structure change occurs in TMMA and SSQXN-8 resins. Also the lowest values of ΔS^* (−179.29 to −166.04 J mol^{-1} K^{-1}) support the higher stability and hence, the least steric difference of the system. These results are parallel to that reported for other inorganic ion exchangers.[23,30]

CONCLUSION

N, N, N\, N-tetramethylmalonamide and silsesquioxane resins were synthesized with different polymerization routes and characterized. Their structure was instrumentally revealed via elemental analysis, FTIR, ^{1}H-NMR, and ^{13}C-NMR spectroscopic analyses. During the study of their sorption behavior toward Nd^{+3}, Eu^{+3}, and Gd^{+3} ions, as trivalent lanthanides that may exist in different waste compositions, superfast kinetics were observed; low equilibrium profiles and low activation energies were obtained.

The exchange kinetics of Nd^{+3}, Eu^{+3}, and Gd^{+3} ions on TMMA and SSQXN-8 were studied as a function of particle radius, and reaction temperatures. The rate of exchange was independent of the metal ion concentration, which proves that the conditions set in this work fulfill particle diffusion mechanism for the investigated metal ions.

The rate of exchange increased with decreasing the particle size, whereas it increased with increasing the reaction temperature.

Negative ΔS^* values were obtained and revealed that the investigated metal ions were sorbed on TMMA and SSQXN-8 in the unhydrated form.

The authors gratefully acknowledge Prof. Dr. I. M. Ismail, chemical engineering department, Cairo University, Cairo, Egypt, for his literature scientific support during preparation of TMMA resin.

References

1. Rao, L.; Zanonato, P. L.; Bernardo, P. D.; Bismondo, A. Inorganica Chim Acta 2000, 306, 49.
2. Filho, N. L. D.; Costa, R. M.; Marangoni, F. Colloids Surf A: Physicochem Eng Aspects 2008, 317, 625.
3. Waddon, A. J.; Coughlin, E. B. Chem Mater 2003, 15, 4555.
4. Phillips, S. H.; Haddad, T. S.; Tomczak, S. J. Curr Opin Solid State Mater Sci 2004, 8, 21.
5. International Atomic Energy Agency (IAEA). Application of ion exchange processes for the treatment of radioactive waste and management of spent ion exchangers, technical reports series, No. 408, IAEA, Vienna, 2002.
6. Nogami, M.; Ismail, I. M.; Yamaguchi, M.; Suzuki, K. J Solid State Chem 2003, 171, 353.
7. Nogami, M.; Sakashita, T.; Yuki, M.; Shirato, K.; Ikeda, Y. Proceedings of the 12th Pacific Basin Nuclear Conference (PBNC2000); Seoul, Korea, 2000; 477–483.

8. Nogami, M.; Ikeda, Y.; Shirato, K.; Ito, M.; Sakashita, T. Autumn Meeting, Atomic Energy Society of Japan, J17; September 2000; 608.
9. Kim, S.; Tomiyasu, H.; Ikeda, Y. J Nucl Sci Technol 1998, 35, 163.
10. Haddad, T. S.; Viers, B. D.; Phillips, S. H. J Inorg Organomet Polym 2001, 11, 155.
11. Huesing, N.; Brandhuber, D.; Kaiser, P. J Sol-Gel Sci Techn 2006, 40, 131.
12. Ismail, I. M.; Masanobu, N.; Kazunori, S. Sep Purif Technol 2003, 31, 231.
13. Lide, D. R., Ed.CRC Handbook of Chemistry and Physics; CRC Press: California, 2004.
14. Marczenko, Z. Spectrophotometric Determination of Elements; Ellis Harwood Ltd.: Poland, 1976.
15. El-Gammal, B.; Ibrahim, G. M.; El-Nahas, H. H. J Appl Polym Sci 2006, 100, 4098.
16. Li, G. Z.; Wang, L.; Ni, H.; Pittman, C. U. J Inorg Organomet Polym Mater 2001, 11, 123.
17. Shady, S. A.; El-Gammal, B. J Colloids Surf 2005, 268, 7.
18. Hegazy, E. A.; El-Gammal, B.; Khalil, F. H.; Mabrouk, T. M. J Appl Polym Sci 2006, 102, 320.
19. Ibrahim, G. M.; El-Gammal, B.; Mowafy, E. A. Arab J Nucl Sci Appl 2004, 37, 93.
20. Khalil, T.; Abou El-Nour, F.; El-Gammal, B.; Boccaccini, A. Powder Technol 2001, 114, 106.
21. Helfferich, F.Ion Exchange; Dover: New York, 1995.
22. Barrer, R. M.; Bartholomew, R. F.; Rees, L. V. C. J Phys Chem Solids 1963, 24.
23. El-Naggar, I. M.; Mowafy, E. A.; Abdel-Galil, E. A. Colloids Surf A: Physicochem Eng Aspects 2007, 307, 77.
24. El-Naggar, I. M.; El-Absy, M. A.; Aly, S. I. Solid State Ion 1992, 50, 241.
25. El-Naggar, I. M.; Aly, H. F. Solvent Extr Ion Exch 1992, 10, 145.
26. El-Naggar, I. M.; Al-Absy, M. A. J Radioanal Nucl Chem Articles 1992, 157, 313.
27. El-Naggar, I. M.; Zakaria, E. S.; Shady, S. A.; Aly, H. F. Solid State Ion 1999, 122, 65.
28. Jeanjean, J.; Piriou, B.; Fedoroff, M.; Bercis, L. J Colloid Interface Sci 1997, 149, 440.
29. Mallah, M. H.; Shemirani, F.; Ghannadi Maragheh, M. J Radioanal Nucl Chem 2008, 278, 97.
30. El-Naggar, I. M.; El-Dessouky, M. I.; Aly, H. F. Solid State Ion 1992, 57, 339.